Study of near SOL temperature and density gradient lengths with Thomson Scattering

HJ. Sun[1], E. Wolfrum[1], T. Eich[1], B. Kurzan[1], S. Potzel[1] and the ASDEX Upgrade Team

Max Planck Institute for Plasma Physics, Boltzmannstr. 2, 85748 Garching, Germany

E-mail: sunhj@ipp.mpg.de

Abstract. Improvements to the Thomson Scattering diagnostic have enabled the study of near scrape-off layer (SOL) decay lengths in the 2014 ASDEX Upgrade experimental campaign. A database of H-mode discharges has been studied using a two-line fit method for the core and log-linear fit for the near SOL region under both attached and detached divertor conditions. SOL electron temperature T_e profiles have been found to have a radial exponential decay distribution and which does not vary poloidally, consistent with the two-point model. In attached H-mode regimes, a log-linear regression shows that the SOL upstream dataset has the same main parametric dependencies as the scaling inferred from downstream Infrared camera measurements. A simple collisional relation from two-point model is found to best relate the upstream decay lengths and downstream divertor power widths. The SOL T_e gradient length appears to be independent of T_e pedestal parameters, but may correlate with the pedestal electron pressure parameters. Both the pedestal and SOL density and temperature scale lengths are linearly correlated with an almost constant gradient ratio, η_e. The smaller gradient ratio η_e and the fact that the Spitzer-Härm model is more valid, agrees with the studied plasma lying in the highly collisional regime. The high density transition in L-mode plasmas as reported in many machines has been observed in AUG detached H-mode regimes. When the flattening of density profile happens in H-mode detached plasma, the broadening of near SOL T_e decay length $\lambda_{T_{e,u}}$ also appears which may be good news for the future machine.

PACS numbers: 52.25.Fi, 52.50.Gj

1 Introduction

A major constraint in the design of fusion power plants is the maximum heat flux to the divertor targets. Thus, predicting this heat flux is a critical part of the physics basis for future devices. The power providing this heat flux originates in the core plasma and transfers across the separatrix into the open flux surface region known as the Scrape-off Layer (SOL). In the SOL, the heat flows poloidally, from the upstream to the divertor target, as well as radially [1] [2]. The radial extent of the SOL is usually small - on the millimeter scale.

Studies of Infrared (IR) camera measurement of the power flux in the divertor target regions of six tokamaks JET, DIII-D, ASDEX Upgrade, C-Mod, NSTX and MAST [3] [4] [5] [6] [7] have shown

that the observed divertor heat flux is consistent with a model where an upstream exponentially radially decaying heat flux profile diffuses along and perpendicular to the field lines in the divertor to the divertor target. A regression analysis based on the resulting multi-machine database for the upstream high confinement mode (H-mode) SOL power fall-off length, $\lambda_{q\|e}$, has shown that the most important scaling parameter is the poloidal magnetic field (or equivalently the plasma current), with $\lambda_{q\|e}$ decreasing linearly with increasing B_{pol}. In these studies, an exponentially decaying radial profile for the parallel heat flux was assumed at the divertor entrance with radial width, $\lambda_{q\|e}$ [8]. Power flow in the divertor region is assumed to be broadened by perpendicular heat diffusion and perpendicular diffusion is included by introducing a Gaussian, with a width S. Further, an empirical parametric scaling (Eich scaling: see Table III of Reference [3]) of $\lambda_{q\|e}$, measurements found them to be well described by:

$$\lambda_{q\|e} = (0.73 \pm 0.38) B_T^{-0.78\pm0.25} q_{\mathrm{cyl}}^{1.20\pm0.27} P_h^{0.1\pm0.11} R_{geo}^{0.02\pm0.2}. \quad (1)$$

Here, $\lambda_{q\|e}$ is measured in mm; B_T is the toroidal magnetic field, measured in Tesla; q_{cyl} is the cylindrical safety factor; P_h is the heating power, measured in MW; and R_{geo} is the geometric radius of the plasma, measured in metres. When the scaling is applied to ITER for the H-mode burning plasma scenario at $I_p = 15$ MA, a heat flux width of ≈ 1 mm results, significantly lower than the previous projected width of ≈ 5 mm [3].

Detached plasma regimes are attractive for fusion machines since erosion and melting of target surfaces are reduced. Due to the constraints of IR cameras, the measurements used to establish the Eich scaling come from inter-ELM periods in attached divertor discharges over a limited range of operating parameters compared to conditions expected in fusion power plants and ITER at high performance. Thus, upstream decay lengths provide important complementary information to divertor measurements, particularly in detached and partially detached discharges.

This paper focuses on upstream measurements of the electron density and temperature from the Thomson Scattering system on the ASDEX Upgrade (AUG) tokamak to test whether the Eich scaling correctly predicts the upstream fall off length. Two-point models provide simple relations between upstream density and temperature widths in the scrape-off layer and the power width in attached divertor [1] [2]. Making the usual assumption that plasma transport is that of a classical fluid and electrons and ions are thermally coupled, the parallel (along magnetic field line) electron heat flux, $q_{\|e}$, can be expressed as

$$q_{\|e}^{Spitzer} = -\kappa_{0e} T_e^{5/2} \frac{\partial T_e}{\partial x}. \quad (2)$$

Here, κ_{0e} is the Spitzer–Härm electron heat conduction, T_e is the electron temperature, and x is the spatial coordinate along the field line. However, in the weakly collisional regime this expression must be modified by the inclusion of a flux-limited parallel electron heat flux [9]:

$$\frac{1}{q_{\|e}} = \frac{1}{q_{\|e}^{Spitzer}} + \frac{1}{q_{\|e}^{flux-limited}}. \quad (3)$$

Here, $q_{\|e}^{flux-limited} = \alpha n_e v_{te} k T_e$. Here α is a constant flux-limited parameter and v_{te} is the thermal velocity.

Defining s as the radial spatial coordinate, which is perpendicular to the field line, and assuming an exponentially decaying radial profile for the parallel heat flux, as posited in the previous IR studies [3], the upstream electron temperature profile can be expressed as

$$T_{e,u} = T_{e0,u} \cdot exp\left(-s/\lambda_{T_{e,u}}\right), \tag{4}$$

with $\lambda_{T_{e,u}}$ being the width of the upstream SOL electron temperature profile. Thus, for the strongly collisional regime, the upstream electron heat flux width can be related to the upstream SOL electron temperature width by the expression

$$\lambda_{q_{\|e}^{Spitzer},u} = \frac{2}{7}\lambda_{T_{e,u}}, \tag{5}$$

The equivalent relation in the very weakly collisional regime [9] is

$$\lambda_{q_{\|e}^{flux-limited}} = \left(\frac{3/2}{\lambda_{T_e,u}} + \frac{1}{\lambda_{n_e,u}}\right)^{-1}, \tag{6}$$

with $\lambda_{n_e,u}$ being the width of the upstream SOL electron density profile.

For the strongly collisional regime, with the assumption that all of the power enters the SOL in a poloidally localized but fairly broad region around the midplane upstream of the divertor, Equation (2) may be integrated. Making the additional assumption that the upstream $T_{e,u}$ is larger than that at the target, gives

$${T_{e,u}}^{7/2} \approx \frac{7q_{\|e,u}L_c}{2\kappa_{0e}}. \tag{7}$$

Here, L_c is the connection length.

This paper exploits upstream measurements of the electron density and temperature from the ASDEX Upgrade tokamak to study the relation between upstream decay lengths and divertor power widths, and to test whether the scaling of upstream decay lengths agrees with the one based only on downstream IR camera measurements. In addition, the upstream profiles in plasmas with detached divertors are studied. The rest of this paper is organized as follows. The recently upgraded high-resolution Thomson scattering system is introduced in section 2. The two-line fit and log-linear fit methods used in the paper are also introduced. In section 3, the T_e profile features observed in AUG attached H-mode discharges are discussed and the most important regression results are given. Results from partially and fully detached plasmas are then presented in section 4. Finally, in section 5, the results are summarized and discussed together with the future plans for this work.

2 Experimental Method

2.1 Thomson scattering system

In ASDEX Upgrade, high-resolution electron temperature and density profiles can be obtained simultaneously by a vertical Thomson Scattering (TS) system [10]. The scattering volumes of the TS system are illustrated in Figure 1. The system is equipped with 4 Nd: YAG lasers at 1064 nm for core profiles and 6 lasers for the edge plasma. The lasers run at 20 Hz each, with an adjustable delay time

between them. Normally, they are equally spaced in time, forming an 80 Hz pulse sequence for the core and 120 Hz for the edge. All 10 lasers are launched vertically from the bottom of AUG and the scattering volumes of both the edge TS and the core TS have a length of 25mm. They are imaged directly through air to the polychromators which form a profile with 16 channels for the core and 11 channels for the edge. The actual spatial resolution of the TS system in the outer mid-plane of the plasma is determined by mapping the scattering volumes (length 25 mm) to this spatial position, with a spatial resolution of 25 mm for the core and of around 3 mm for the edge. Several improvements to the edge TS system were made in 2013: better alignment between lasers and polychromators, accomplished by new mounts for the polychromators, corrected objective lens, and deeper penetration into the edge plasma due to an inward shifted laser position. Due to these improvements, significantly better quality edge measurements have been achieved in the 2014 experimental campaign, which enables the study of the T_e decay length, $\lambda_{T_{e,u}}$, across the separatrix. Figure 2 shows a typical T_e profile from the TS system for a type-I ELMy H-mode discharge on AUG. Since this study will focus on the near SOL region, edge profile analysis is made carefully. As illustrated in Figure 1, the edge T_e profile is actually a combination of two profiles in two different positions. So, profiles above and below the mid-plane can be obtained for every single discharge, as shown in Figure 2. In the figure, the red profile is the one from below the mid-plane and the black above the mid-plane. There is no obvious difference between the two profiles and this is checked to be common in all analyzed discharges in this paper. The power width scaling used here for comparison was generated by careful analysis of thermography data from several machines. The experimental description of IR camera on AUG can be found in [11].

The profile analysis is performed with composite ELM synchronized profiles in attached regimes. Data are accumulated over steady state plasma phases of duration 0.5–1.0 seconds (including ELMs) where the global plasma parameters were constant. The data used for the gradient lengths study is synchronized in time relative to the onset of an ELM by using the divertor current signal. The relevant period for profile synchronization is defined from −3.5 to −1.5 ms relative to the ELM onset time, but at least 4 ms after the previous ELM. At large radius density becomes low and uncertainties on T_e measurements become comparable to the measurements themselves. Further, significant spikes in T_e are observed which are believed to be due to transient effects such as filaments.

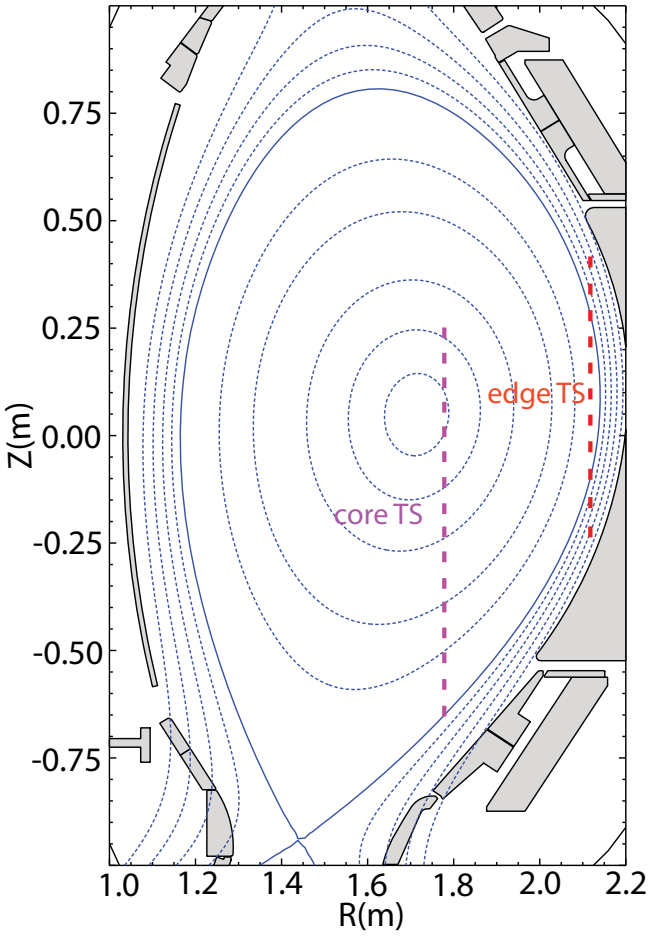

Figure 1. Poloidal cross-section of ASDEX Upgrade for a typical H-mode discharge showing the edge (red dashed) and core (magenta dash dotted) Thomson scattering volumes.

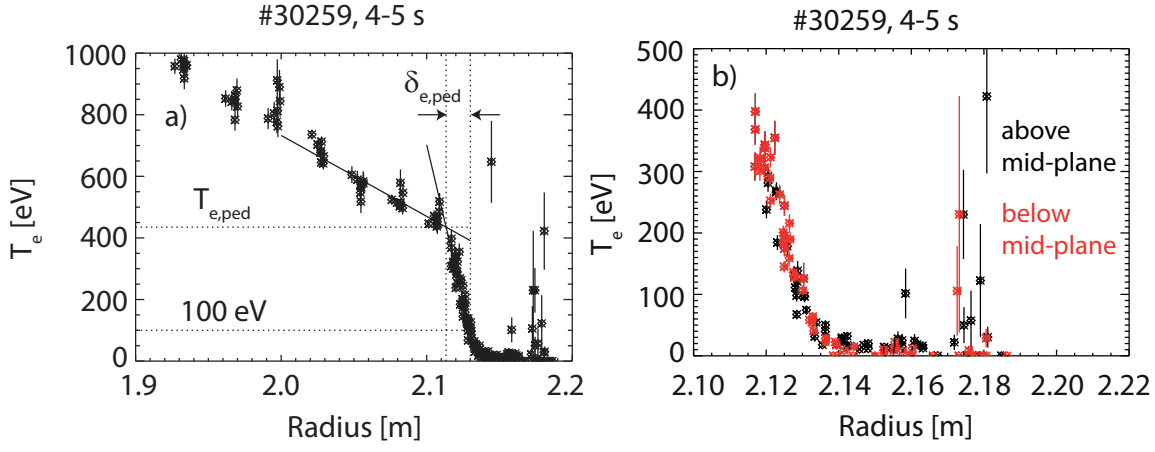

Figure 2. Shot #30259, a typical T_e profile from TS of AUG type-I ELMy H-mode discharge for: (a) the pedestal-SOL region and (b) just the SOL region. The horizontal coordinate is the major radius on the midplane. Core TS data is shown in black. Edge TS data is shown in black (above midplane measurement) and red (below midplane measurement). The two edge TS measurements are approximately 30° apart poloidally. In Figure 2(a), the two line fit is shown overlaid (solid line) with the pedestal top and bottom identified by the dashed lines.

2.2 Two-line fit and log-linear fit

The two-line fit method has been tested with both simulated and experimental data to show better reproducibility of pedestal parameters than other fitting methods [12]. In this paper, the two-line fit method described in Reference [12] [13] will be used to determine plasma pedestal parameters, which include the electron temperature pedestal gradient; the electron temperature at the pedestal top, $T_{e,ped}$; and the pedestal width, $\delta_{e,ped}$; as illustrated in Figure 2(a). A previous study shows that a temperature of around 100 ± 20 eV at the separatrix is predicted for devices like AUG [14]. Based on this, in common with similar previous studies, in this analysis the separatrix position will be estimated as the point where $T_e = 100$ eV.

As discussed in Section 1, in previous studies of the SOL power decay length based on downstream IR measurements, a purely exponential radial decay of the parallel energy transport was assumed at the divertor entrance [3]. To examine whether this exponential profile is applicable in this upstream λ_{T_e} study, edge T_e profiles are plotted on a log-linear scale. A log-linear plot of the same data shown in Figure 2(b) is shown in Figure 3. The profile in the figure is clearly consistent with an exponential radial decay in the near SOL region in both temperature and pressure profiles, and such an exponential profile is found to be consistent with all the analyzed discharges on AUG. Based on this fact, the upstream T_e decay length $\lambda_{T_{e,u}}$, density decay length λ_{n_e} and pressure decay length λ_p can be evaluated by a log-linear fit in the near SOL region, as illustrated in Figure 3 with a solid line. Here, as discussed, a temperature of 100 eV (ln 100 ≈ 4.6) is used to determine the separatrix position. The outer most point used for fitting is that at which error bars become comparable to the measured T_e.

The density and temperature gradient lengths, $L_{T_e} = \{\partial ln(T_e)/\partial s\}^{-1}$ and $L_{n_e} = \{\partial ln(n_e)/\partial s\}^{-1}$ and their ratio $\eta_e = L_{n_e}/L_{T_e} = \partial ln(T_e)/\partial ln(n_e)$ are important in transport physics and determine turbulence characteristics. Since the TS diagnostic measures the electron temperature and density profiles at exactly the same spatial and temporal points, a log-log plot of T_e profile versus n_e profile (Figure 4) can be used to determine the gradient ratio η_e [15].

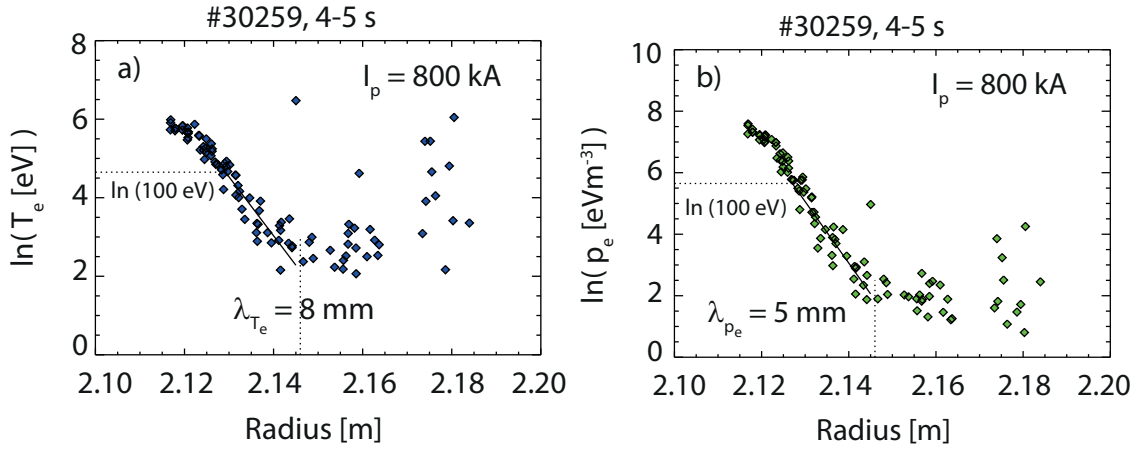

Figure 3. Log-linear plot of the electron temperature (a) and electron pressure (b) against major radius on the midplane for discharge #30259, with a fitted line (solid line) in the near SOL. The dashed lines identify the region over which the fit is made: from the separatrix to the radius at which error bars become comparable to the measured T_e. Data shown is time points with ELM synchronized between 4 and 5 seconds from the start of the discharge. The slope of the fitted line gives the decay lengths.

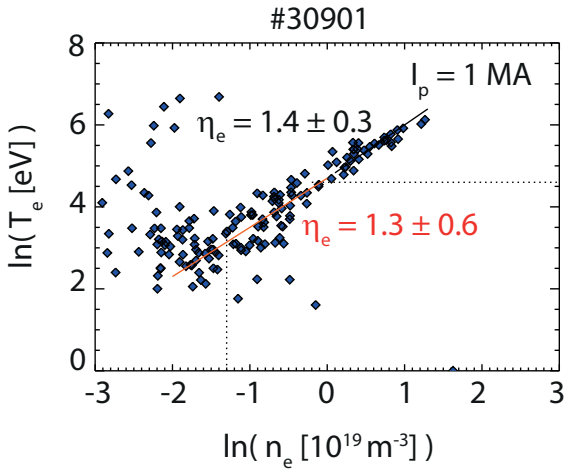

Figure 4. Log-log plot of electron temperature versus density. The (solid) line fit to pedestal (black) and near SOL (red) data gives the gradient ratio η_e. The dashed lines identify the region over which the fit for the near SOL is made, equivalent to the region from the separatrix to the radius at which error bars become comparable to the measured T_e.

3 Experimental results under attached divertor conditions

3.1 Discharges database

Since the measurements used to establish the Eich scaling come from type-I ELMy H-mode discharges in attached divertor discharges, a database with similar plasma conditions in the 2014 AUG campaign was constructed to study upstream near SOL gradient lengths. Table 1 shows an overview of the key plasma parameters. In the table, I_p is the plasma current, B_T the toroidal magnetic field, q_{95} the edge safety factor, P_h the heating power, and f_{GW} the Greenwald density fraction. The geometric radius of the plasma, R_{geo}, which is included in the multi-machine scalings does not vary greatly within the database, so size scaling is not considered in this paper. One should also keep in mind that this dataset contains limited B_T. Although B_T varies from 1.9 to 2.5 T, over 80% discharges are around 2.5 T which causes larger uncertainties just as the scaling result of λ_q from IR camera and H-mode $\lambda_{T_e,u}$ scaling with TS system

Table 1. Range of key parameters in the database of analyzed discharges

I_p [MA]	B_T [T]	q_{95}	P_h [MW]	f_{GW}
0.6-1.2	1.9-2.5	3.5-7	5-15	0.45-0.6

3.2 Upstream profile features

As mentioned in section 2, there are two key features observed in the upstream profiles of the AUG dataset. Since both of them are very important for the further analysis in this paper, they are repeated here. As shown in Figure 2, the independently measured upper and lower profiles of the SOL electron temperature, which are about 30° apart poloidally, show no significant difference for any discharge in the dataset. Thus, the assumption that all of the power enters the SOL in a poloidally localized but fairly broad region around the midplane upstream of the divertor, is consistent with the dataset. Log-linear plots of upstream profiles show that a purely exponential radial decay can be applied in the

power exhaust analysis in near SOL region, as shown in Figure 3. The exponential distribution yields a direct measurement of gradient lengths which is applied widely in this paper.

3.3 Regression results of T_e decay length, $\lambda_{T_e,u}$

In this section, the dataset of Section 3.1, is used and standard numerical tools are applied for log-linear regression with the form $\lambda_{T_{e,u}} = C \cdot B_T^{C_B} \cdot q_{cyl}^{C_q} \cdot P_h^{C_P} \cdot R_{geo}^{C_R}$. The coefficient of determination, R^2 (R^2=1 means perfect fit), will be used as a measure of the quality of the regression result. Before making the empirical regression, the dependence of $\lambda_{T_{e,u}}$ on some primary parameters is presented. A strong dependence on plasma current I_p is found, Figure 5(a). $\lambda_{T_{e,u}}$ decreases when the plasma current increases, which is consistent with the result of the $\lambda_{q_{\|e,u}}$ dependence. In the figure, different colors demonstrate different plasma currents. With $I_p = 600$ kA, the obvious gap between discharges (red asterisk) is due to the different q_{95}, as can be seen from Figure 5(b), where the same data are plotted against q_{95}. There is no obvious dependence on heating power within the accuracy of the measurements, this is shown in Figure 5(c) where only data from discharges with $I_p = 1$ MA are chosen. A regression analysis of $\lambda_{T_{e,u}}$ with the same parameters as used in the 'Eich' scaling (equation 1) gives

$$\lambda_{T_{e,u},reg} = (2.63 \pm 1.37) B_T^{-0.50\pm0.67} q_{\mathrm{cyl}}^{0.974\pm0.17} P_h^{0.05\pm0.23}, \tag{8}$$

see Figure 6. Here, $\lambda_{T_{e,u},reg}$ is in mm, B_T is in Tesla, and P_h is in MW. The regression has a fit quality of R^2=0.76. As will be shown in the section 3.6, the simple Spitzer-Härm relation $\lambda_{q_{\|e,u}} = \frac{2}{7}\lambda_{T_e,u}$ can be used to relate the upstream gradient length to the decay width of the power flux entering the diverted region. Since density gradient lengths are needed for the study of upstream-downstream relation, a detailed comparison will be presented in section 3.6. A comparison between $\frac{2}{7}\lambda_{T_{e,u}}$ and $\lambda_{q_{\|e,u}}$ regression results are shown in table 2. As summarized in the table, within uncertainties, the parametric dependences are consistent with Eich scaling[8]. However, it should be emphasized that the B_T dependence has a large uncertainty due to the small variation in B_T across the dataset. Hence, the consistency with B_T dependence is suggestive, but not conclusive. To resolve the dependence further, additional experiments should be performed which extend the range of B_T.

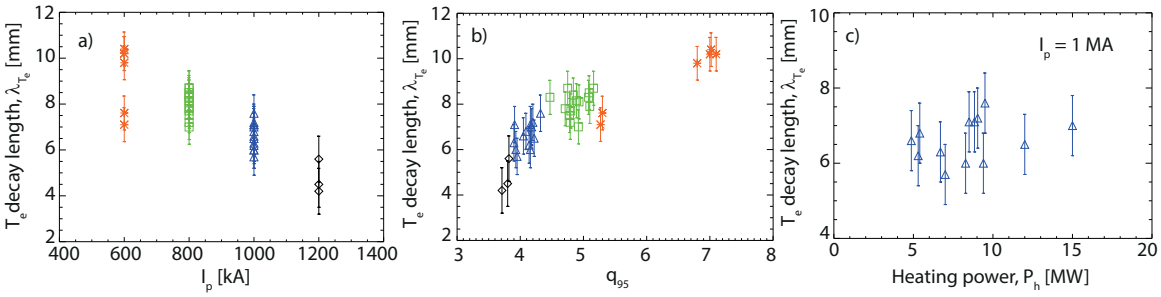

Figure 5. SOL T_e decay length $\lambda_{T_{e,u}}$ for AUG type-I ELMy H-mode dataset of Section 3.1 against: (a) plasma current; (b) edge safety factor, q_{95}; and (c) heating power. Different colors indicate different plasma currents.

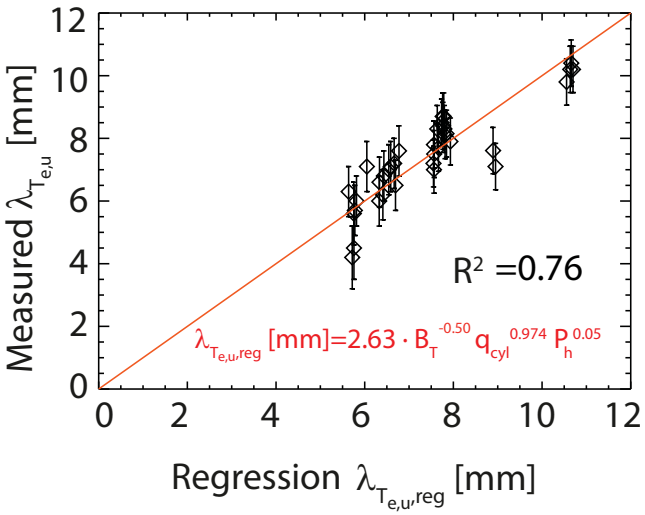

Figure 6. Upstream T_e decay length, $\lambda_{T_{e,u}}$, against the scaling derived from a log-linear regression method, Equation 8.

Table 2. Comparison of regression results between λ_{T_e} and $\lambda_{q_{\parallel e}}$

		C_0	C_B	C_q	C_P	R^2
Multi-machine, IR data [3]	$\lambda_{q_{\parallel e,u}}$	0.73±0.38	-0.78±0.25	1.20±0.27	0.10±0.11	0.80
AUG , IR data [4]	$\lambda_{q_{\parallel e,u}}$	0.78±0.69	-0.63±1.05	1.14±0.81	-0.05±0.31	0.43
AUG, TS data (Equation 8)	$\frac{2}{7}\lambda_{T_{e,u}}$	0.73±0.39	-0.50±0.67	0.97±0.17	0.05±0.23	0.76

3.4 Pedestal-SOL correlation study

As discussed in Section 1, one of the main theoretical explanations for the scaling of the SOL heat flux width is through a critical gradient model. To investigate the consistency of the dataset of Section 3.1 with such a model, the correlation between decay length and pedestal gradients was studied. Figure 7(a) and Figure 7(b) show the $\lambda_{T_{e,u}}$ dependence on pedestal top temperature and temperature gradient. Within the accuracy of the measurements, there is no obvious correlation between the T_e pedestal parameters and the SOL T_e decay length, either with same current or including all currents. The correlation between $\lambda_{T_{e,u}}$ and pedestal top pressure is illustrated in Figure 7(c). Although there is a clear negative correlation between the T_e SOL decay length and the pedestal top pressure, there is no evidence of such a trend within data taken for a single plasma current. This suggests that the $\lambda_{T_{e,u}}$-$p_{e,ped}$ correlation is a consequence of both parameters depending on plasma current rather than a direct dependence of one on another. A similar behavior is found for the correlation between the SOL T_e decay length and the pedestal p_e or T_e gradient, as shown in Figure 7(b) and Figure 7(d). In both cases a negative correlation is seen, but the same tendency is not observed within datasets restricted to a single plasma current. The difference between temperature and pressure pedestal dependence can also be seen in Figure 8(a) and Figure 8(b). In Figure 8(a), both discharges have the same plasma current, $I_p = 1$ MA, but one discharge has a pedestal top T_e that is about 100% larger than the other and a pedestal T_e gradient that is about 90% steeper than the other. However, the SOL T_e decay length, λ_{T_e}, is almost the same and within the measurement uncertainties - one being 6 mm and another 6.6 mm, with an error bar of about 10% in both cases. However, for the same discharges, the pedestal top electron

pressure of one discharge is only 50% higher than the other and the pedestal electron pressure gradients are the same within measurement errors. These results show that the SOL T_e decay length does not correlate with pedestal T_e or its gradient, but seem to correlate with the pedestal electron pressure gradient. However, the correlation is likely due to both parameters depending on plasma current. The reasons for the higher pressure in discharge #30676 as compared to #30974 are due to higher triangularity ($\delta \approx 0.31$ vs $\delta \approx 0.22$) and higher total heating power (6 MW vs 2.6 MW), despite the lower density ($\overline{n_e} = 6.5 \cdot 10^{19} m^{-3}$ vs $\overline{n_e} = 7.8 \cdot 10^{19} m^{-3}$).

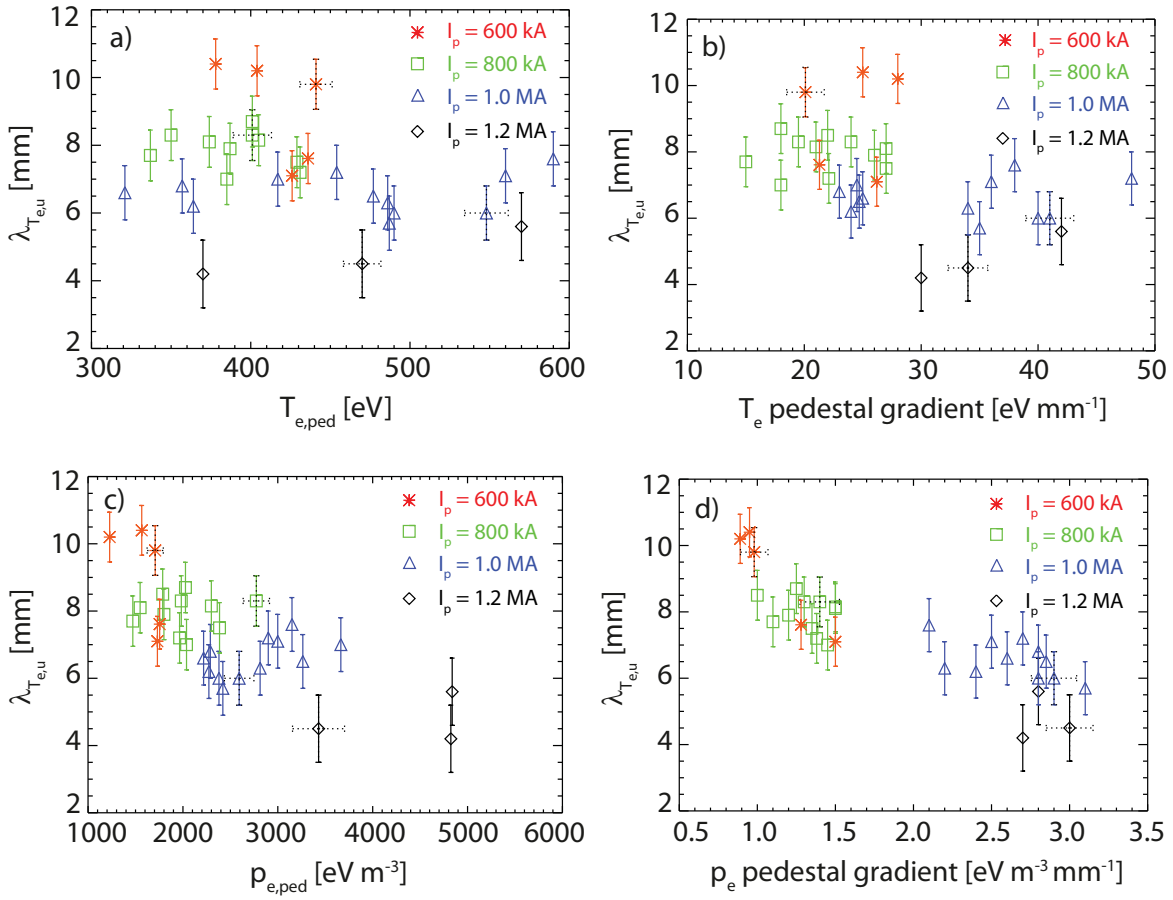

Figure 7. SOL T_e decay length, $\lambda_{T_{e,u}}$, for the type-I ELMy H-mode dataset of Section 3.1 against: a) pedestal top T_e; b) pedestal T_e gradient; c) pedestal top electron pressure; and d) pedestal electron pressure gradient.

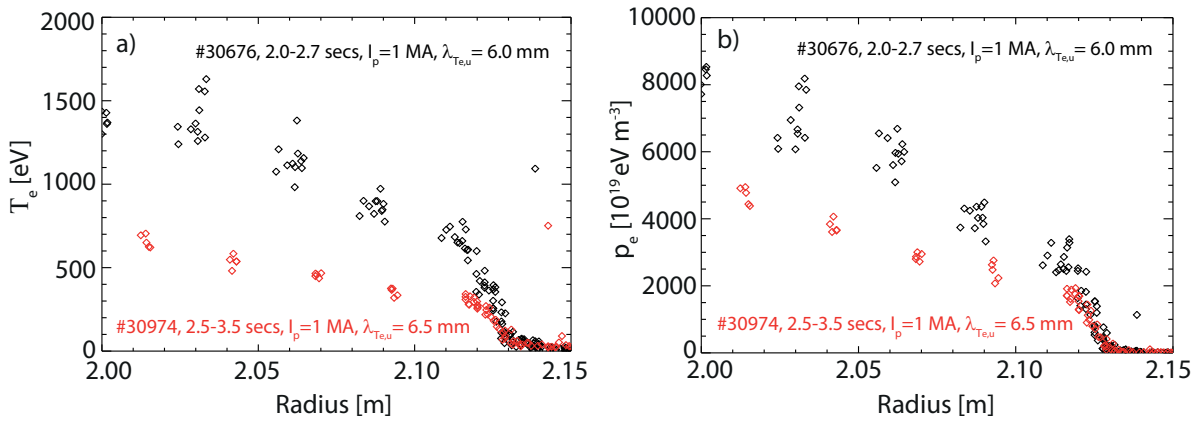

Figure 8. (a) T_e and (b) electron pressure against major radius at the midplane for discharge #30676 and discharge #30974, which are type-I ELMy H-mode discharges with identical plasma currents.

3.5 Density gradient length and gradient length ratio

Using the same method, the density gradient length $\lambda_{ne,u}$ and pressure gradient length $\lambda_{pe,u}$ may also be evaluated. Figure 9 shows the density and pressure gradient lengths against the temperature decay length in the SOL. It can be seen that both $\lambda_{ne,u}$ and $\lambda_{pe,u}$ have an almost linear correlation with $\lambda_{T_{e,u}}$ and $\lambda_{n_{e,u}}$ is roughly 30%-40% larger than $\lambda_{T_{e,u}}$. This motivates the study of the gradient length ratio η_e which is calculated by the method given in Section 2.2. In Figure 10, the black points are η_e in the pedestal region, while the red ones are η_e in the near SOL region. The gradient length ratio is around 1.4 in the pedestal region and smaller in the near SOL with a much larger uncertainty. Within the confidence intervals, the gradient length ratio in the near SOL can be roughly equal to the one in pedestal region. Three discharges with different plasma currents were chosen from the database mentioned above to be plotted as log-log plot in Figure 11. Despite those outliers in the far SOL region, these profiles are parallel with each other and $\eta_e \approx 1.4$ can be calculated from all the discharges. This result is consistent in our chosen database. In the previous studies on AUG, a constant η_e was found to be close to 2 for a series of ELMy H-mode discharges [14] [15]. In a more extensive scaling study [13], the gradient ratio η_e was found to be inversely proportional to collisionality. Thus, the smaller η_e in this paper compared with the earlier study may be due to the higher collisionality of the discharges in the present study. The present dataset has little variation in collisionality, so the dependence of η_e on collisionality cannot be studied here.

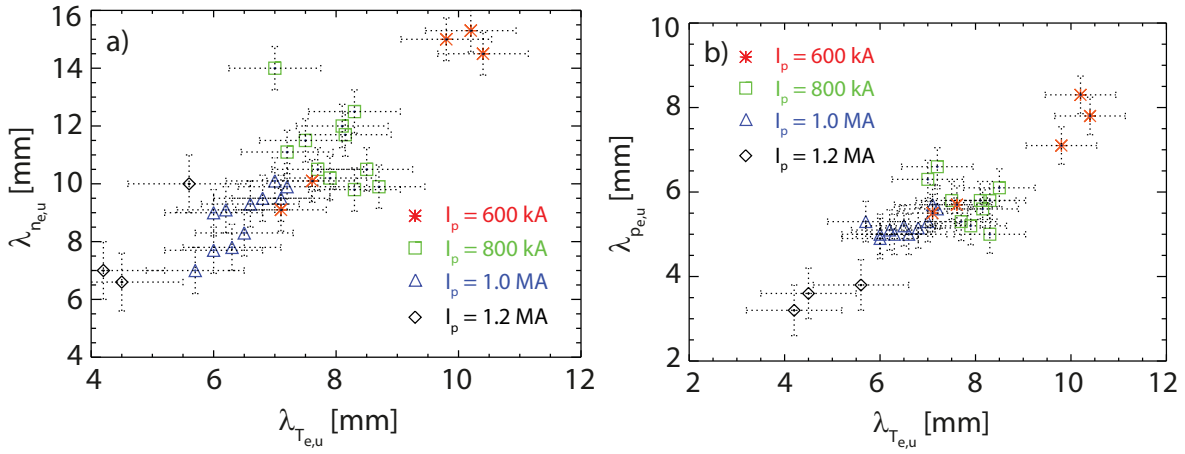

Figure 9. The SOL electron density decay length (a) and SOL electron pressure gradient length (b) against the SOL electron temperature decay length, for the type-I ELMy H-mode dataset of Section 3.1.

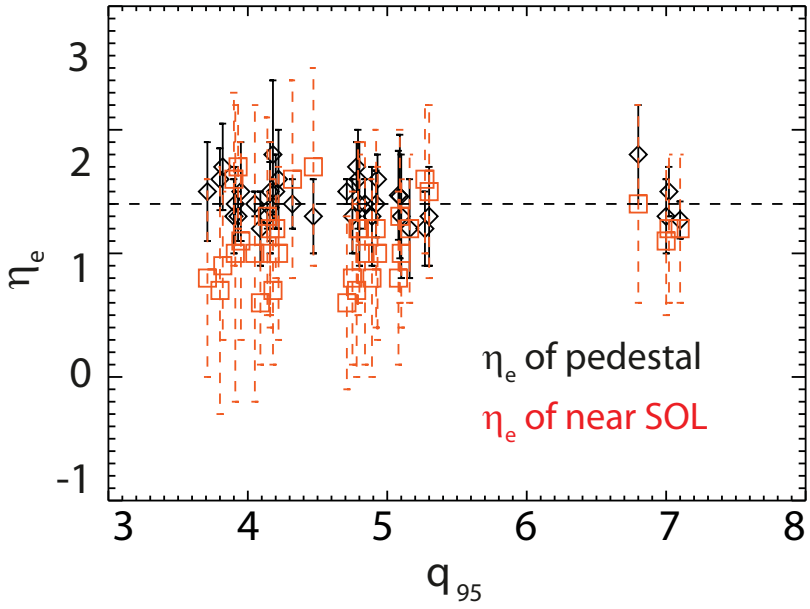

Figure 10. Gradient length ratio η_e plotted against q_{95}. η_e of pedestal region in black and near SOL in red.

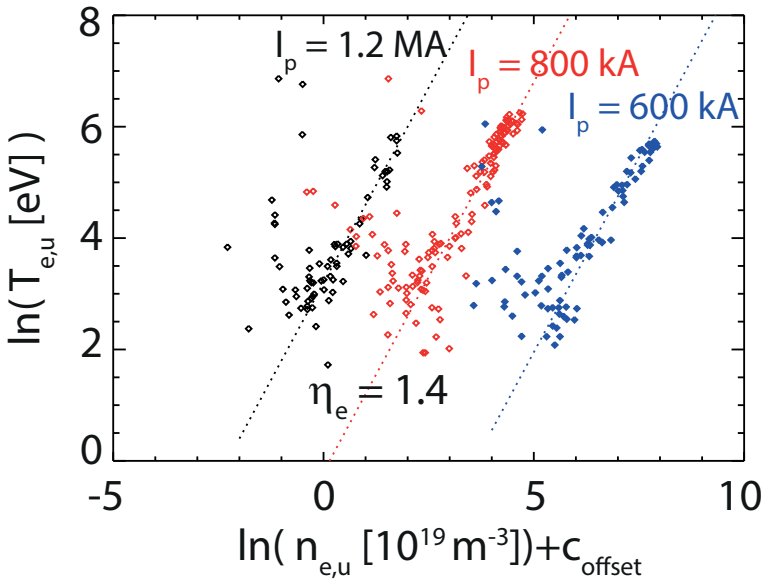

Figure 11. Log-log plot of electron temperature versus density in the edge region for type-I ELMy H-mode attached discharges. Data is for three different plasma currents: 1.2 MA (black), 800 kA (red) and 600 kA (blue). An offset, c_offset, has been introduced in the horizontal coordinate so the trends for the different plasmas currents can be clearly seen. c_offset=0 for 1.2 MA, c_offset=3 for 800 kA, and c_offset=6 for 600 kA.

3.6 The relation between upstream and downstream widths

As discussed in Section 1, the upstream power flux width scalings – such as the 'Eich scaling - derived from downstream IR measurements in the divertor are based on a model with purely diffusive parallel and perpendicular transport in the SOL from the X-point (the entry to the divertor) to the divertor target. By assuming such a model, the upstream SOL power flux profile, which is also assumed to be toroidally symmetric and radially exponential decaying, can be calculated. To relate these

measurements to the upstream electron temperature measurements, $T_{e,u}$, a model for the local SOL transport at the entry to the divertor must be used. The two models that can be considered are Spitzer-Härm diffusion or flux-limited. By using equations 5 and 6, the measurements of the upstream temperature and density measurements discussed in this paper can be mapped to the divertor power decay widths by using each of these models, resulting in the estimated divertor power widths $\lambda_{q_{\|e}^{Spitzer},u}$ and $\lambda_{q_{\|e}^{flux-limited},u}$ respectively. To check which model is more consistent with the AUG dataset, these estimates can then be compared with the 'Eich scaling'. As can be seen in figure 12(a), assuming Spitzer-Härm diffusion results in an estimated divertor power width which agrees well with the estimate based on the downstream IR measurements. However, assuming the flux-limited model, results in an estimated divertor power flux width which is not, figure 12(b), although it is interesting to note that multiplying the 'Eich scaling' by a factor of 1.5 brings the data into agreement, suggesting that the parametric trends are consistent. Thus, for the ASDEX Upgrade type-I ELMy H-mode discharges studied here, a collisional Spitzer-Härm model is more appropriate to relate upstream decay lengths to downstream widths in ASDEX-Upgrade type-I ELMy H-mode discharges.

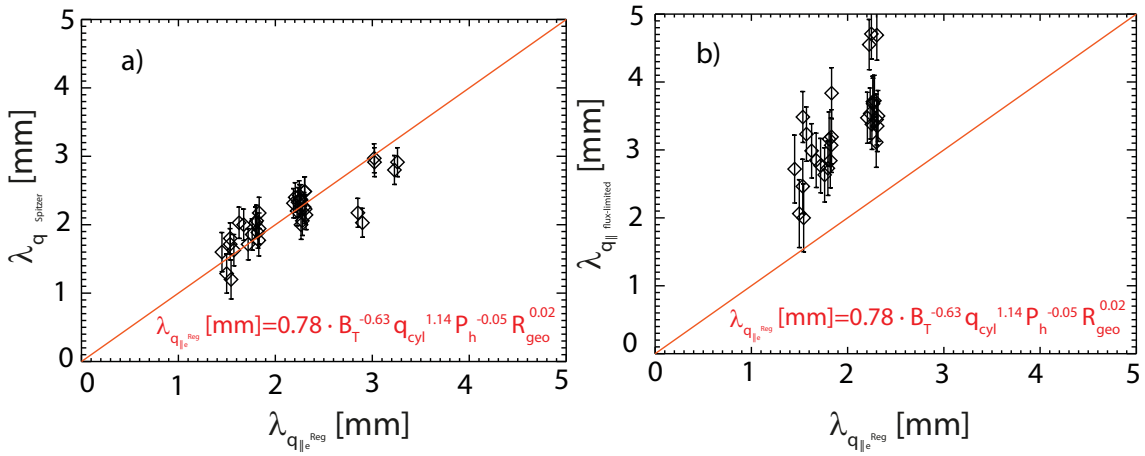

Figure 12: $\lambda_{q,Reg}$ scaling for the divertor power width, derived from downstream IR measurement, versus that derived from the upstream TS measurements and assuming SOL parallel flow is dominated by (a) Spitzer-Härm diffusion, $\lambda_{q,spitzer}$, and (b) a flux-limited model, $\lambda_{q,flux-limited}$.

4 Experimental results under detached divertor conditions

Detached plasma regimes are attractive for fusion machines since erosion and melting of target surfaces are reduced. Due to the constraints of IR cameras, the measurements used to establish the Eich scaling come from inter-ELM periods in attached divertor discharges. Since there is no such instrumental constraints of TS system, the study of upstream decay lengths $\lambda_{T_{e,u}}$ can provide important complementary information for understanding of power exhaust, particularly in detached and partially detached discharges. In this section, the observation of broadening of the upstream decay lengths $\lambda_{T_{e,u}}$ under detached divertor condition will be discussed. To achieve the detached divertor condition, a density scan with fixed current (1 MA) was performed using impurity seeding. A log-linear plot of the same discharge under attached divertor condition is shown in Figure 13(a), with a temperature decay lengths of $\lambda_{T_{e,u}} \approx 6.5\ mm$. While, under detached divertor condition, the temperature decay length is obviously broadened, with $\lambda_{T_{e,u}} \approx 12.5\ mm$, as shown in figure 13(b). The observed decay lengths for

the full density scan are shown in figure 14. Interestingly, the broadening of the temperature decay length $\lambda_{T_{e,u}}$ only happens with completely detached conditions. Partial detachment appears when the Greenwald density fraction f_{GW} is larger than 0.65, while the broadening of $\lambda_{T_{e,u}}$ happens at higher density when f_{GW} is near 0.80 and the divertor is fully detached.

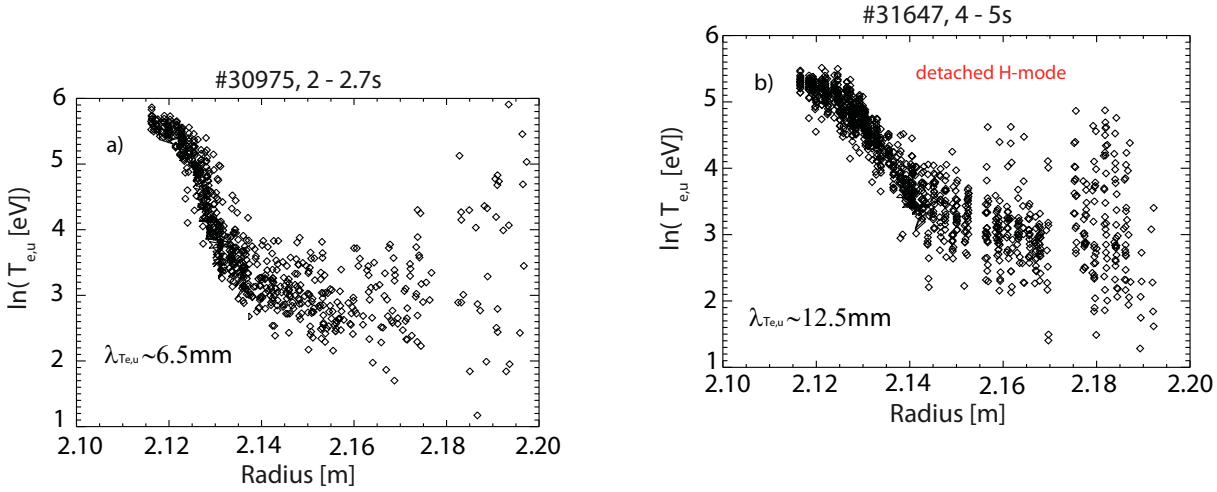

Figure 13. Log-linear plot of the electron temperature against major radius on the midplane for H-mode attached discharge #30975 (a) and H-mode detached discharge #31647. The slope of near SOL profile gives the temperature decay lengths $\lambda_{T_{e,u}}$

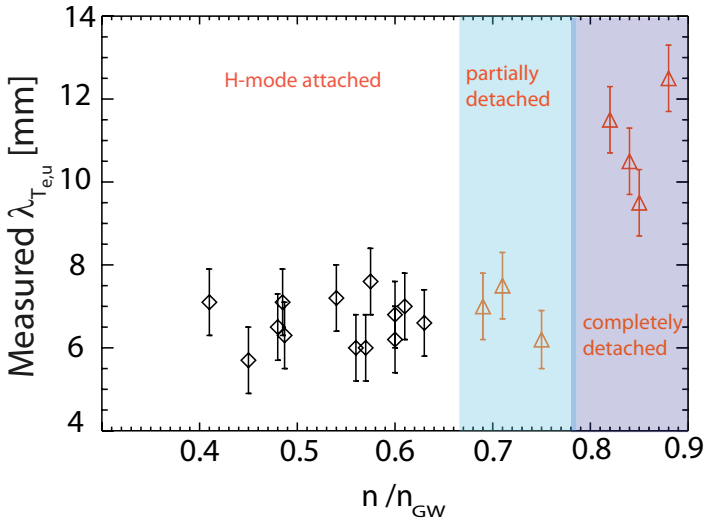

Figure 14. SOL T_e decay length $\lambda_{T_{e,u}}$ for AUG H-mode dataset against greenwald density fraction. Different colors indicate different divertor conditions, white for attached conditions and light blue for partially detached conditions, purple for completely detached regimes.

Turning now to the question of how the electron density profiles vary from detached to attached divertor conditions, Figure 15 shows log-linear plots of the electron density for the same discharges shown in figure 13. Just like the temperature decay length $\lambda_{T_{e,u}}$, the density decay length $\lambda_{n_{e,u}}$ also increases as the divertor becomes detached, with $\lambda_{n_{e,u}} \approx 9\,mm$ under attached divertor condition, while $\lambda_{T_{e,u}} \approx 16.5\,mm$ under detached divertor condition. The variation of the density decay length $\lambda_{n_{e,u}}$ across the whole density scan is illustrated in figure 16. It can be seen that, the flattening of density profile happens after f_{GW} reaches 0.80 and the divertor is fully detached. The feature of density profile flattening in the SOL region has been observed in earlier studies of L-mode plasmas, where the phenomenon has been called the L-mode high density transition (HDT) [16] [17] [18]. After the Greenwald density fraction f_{GW} is larger than a certain value, the density profile in the SOL changes, flattening its gradient and giving rise to a 'shoulder'. Recent studies using Langmuir probe and Lithium beam on AUG show that the value of critical density threshold for the L-mode HDT is about $f_{GW} \approx 0.45$ [19]. Experimental measurements are in good agreement with that this high density transition is related to outer divertor detachment. More recently, a similar phenomenon has been also observed in H-mode operation when f_{GW} is over a critical value which is much larger than the one in L-mode [20]. In further L-mode HDT studies [19], it was found that the collisionality plays key role in the onset of this transition. A similar effective collisionality developed in [21] will be used here to check the critical collisionality for the broadening of near SOL profiles:

$$\nu_*^{eff} = \frac{L_c/C_s}{1/\nu_{ei}} \cdot \frac{\Omega_i}{\Omega_e} \tag{9}$$

Where L_c is the connection length, C_s the sound speed, ν_{ei} the electron–ion collision frequency and Ω_s the gyrofrequency of species s. This effective collisionality ν_*^{eff} can be seen as the ratio between the parallel characteristic length and the ion–electron collision mean free path. As shown in figure 17, the critical value for ν_*^{eff} is about 15.

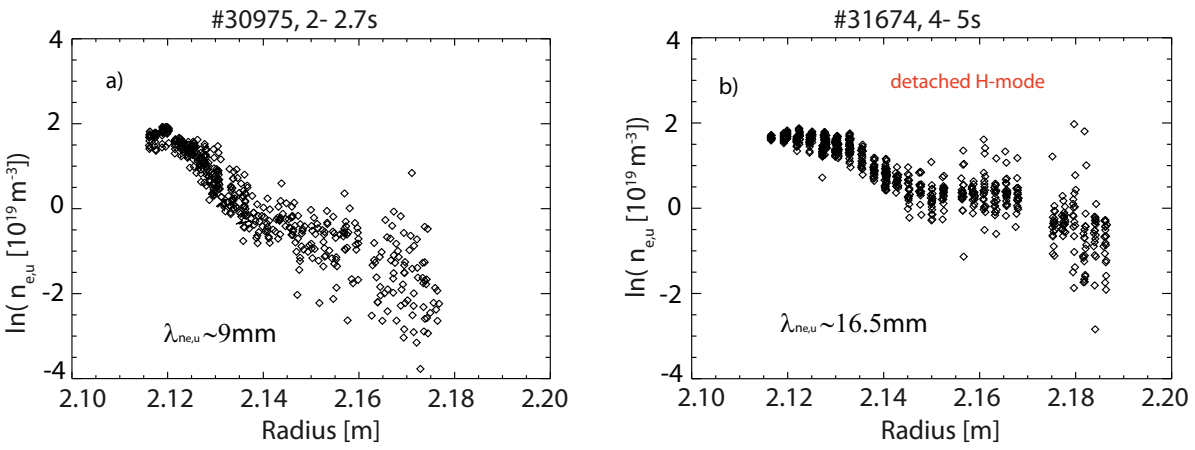

Figure 15. Log-linear plot of the electron density against major radius on the midplane for H-mode

attached discharge #30975 (a) and H-mode detached discharge #31647. The slope of near SOL profile gives the density decay lengths $\lambda_{n_{e,u}}$.

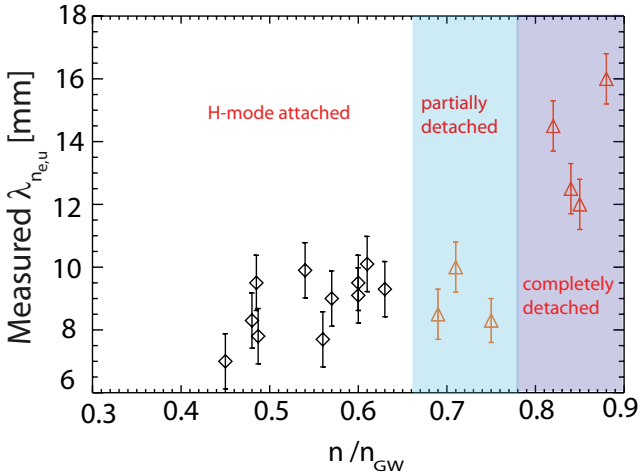

Figure 16. SOL n_e decay length $\lambda_{n_{e,u}}$ for AUG H-mode dataset against greenwald density fraction. Different colors indicate different divertor conditions, white for attached conditions and light blue for partially detached conditions, purple for completely detached regimes.

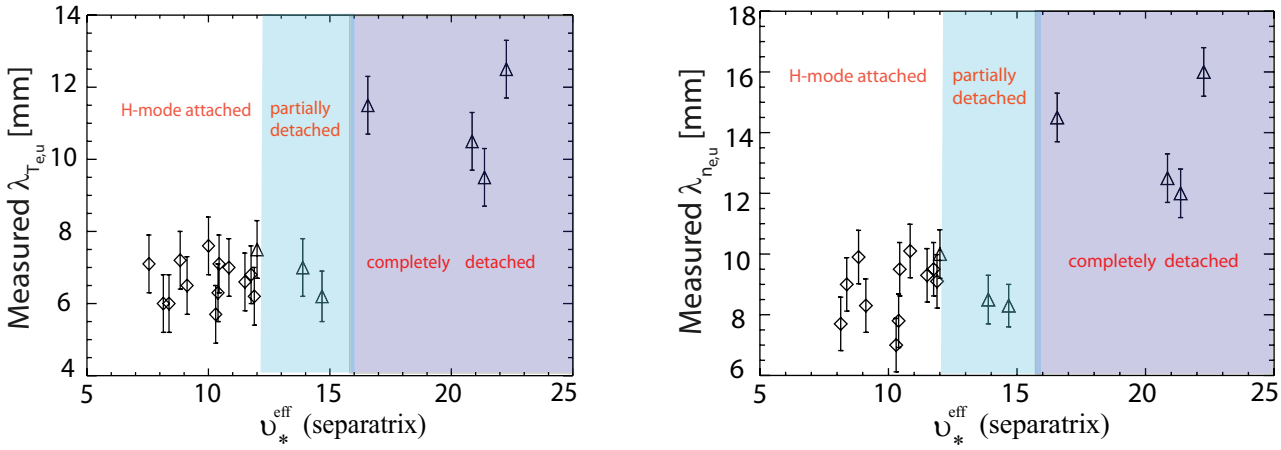

Figure 17. SOL decay length $\lambda_{T_{e,u}}$ (a) and $\lambda_{n_{e,u}}$ (b) for AUG H-mode dataset against effective collisonality ν_*^{eff} . Different colors indicate different divertor conditions, white for attached conditions and light blue for partially detached conditions, purple for completely detached regimes.

5 Summary and discussion

Due to better alignment between lasers and polychromators and corrected objective lens, and deeper penetration into the edge plasma, significantly better quality TS edge measurements have been

achieved in the 2014 ASDEX Upgrade experimental campaign, which enables the study of the T_e decay length, $\lambda_{T_{e,u}}$, across the separatrix. Since the measurements used to establish the 'Eich scaling' [3] come from type-I ELMy H-mode discharges in attached divertor discharges, a database with similar plasma conditions was first constructed to study scaling of upstream near SOL gradient lengths. The dataset has been studied using a two-line fit method for the core and log-linear fit for the near SOL region. The direct profile measurements of AUG type-I ELMy H-mode plasmas show two important features in the edge: SOL T_e profiles have a radial exponential decay distribution; SOL T_e profiles taken at separate poloidal locations above and below the midplane indicate no poloidal variation. A log-linear regression shows that the SOL upstream dataset has the same main parametric dependencies as the 'Eich scaling'. A simple collisional relation from two-point model is found to best relate upstream decay lengths and downstream power widths. Given that the previous scaling was inferred only from downstream measurements using IR data and involved a relatively simple model for the upstream power flux profile and the parallel transport along the field lines and radial transport perpendicular to them, the confirmation of the scaling and assumptions by direct upstream measurements is a significant result. In detached H-mode regimes, the broadening of upstream SOL profiles is observed when the divertor is completely detached.

In attached H-mode regimes, the upstream gradient length $\lambda_{T_{e,u}}$ also has a strong I_p dependence, but several outliers indicate that a q_{95} dependence is more appropriate to describe the gradient length scaling. The SOL T_e gradient appears to be independent of electron temperature pedestal parameters, but may correlate with the pedestal electron pressure parameters. The general trend in the data of "reduced pedestal height" being associated with a flatter pressure profile in the SOL is consistent with C-Mod EDA H-mode results [22]. However, the same tendency is not observed within datasets restricted to a single plasma current. This suggests that the pedestal-SOL correlation is a consequence of both parameters depending on plasma current rather than a direct dependence of one on the other. The density and pressure gradient lengths study shows that the pedestal and SOL density and temperature length scales are linearly correlated, which yields an almost constant gradient ratio $\eta_e \approx 1.4$. In the previous studies on AUG, a constant η_e close to 2 was found for a series of ELMy H-modes [14] [15]. In a more extensive scaling study [13], the gradient ratio η_e was found to be inversely proportional to collisionality. Thus, the smaller η_e in this dataset compared with the earlier study may be due to the higher collisionality of the discharges in the present study. The study of the relation between upstream decay lengths and downstream divertor power width shows that a collisional Spitzer-Härm model is more proper to relate this two regions for the chosen dataset from 2014 AUG campaign, which is consistent with the earlier study on AUG [23]. The result is also consistent with DIII-D result [5], which shows the Spitzer-Härm model is more valid in the high collisional regime. Combining the smaller gradient ratio η_e and the fact that the Spitzer-Härm model is more appropriate, the plasma seems to be in the high collisional regime, with electron and ions highly thermally coupled, in the chosen dataset from 2014 campaign. A physics model is required to provide an understanding as well as to increase confidence in the scaling when it is extrapolated to future devices which may, potentially, lie in different physical regimes. So far, two general classes of models have been considered. The first class of model is the heuristic drift-based model which has been developed by Goldston [24]. A consequence of this model is that the heat flux width should scale as the ion poloidal gyroradius, and, thus, inversely with the plasma current, which is consistent with the empirical scaling. The second class of model is a critical gradient model in which the heat flux width is thought to be set by the separatrix pressure gradient scale length [25] [26] [27]. In these models, turbulence is induced when pressure driven MHD instabilities become unstable and then limit the pressure profile to the 'critical' gradient for the MHD instability. We also compared our data to these models. The

upstream results are not conflict with a heuristic drift wave model. However there is also correlation between upstream decay length and SOL critical gradient. With the present dataset, it is not possible to distinguish between these two models. Thus, these comparison results are not shown in this paper. In the future, a density scan or a B_T scan should be able to separate the two models because there is a separatrix density dependence in the critical gradient model, whereas the HD model has a B_T dependence. Studying a dataset with different collisional regimes will be important for the next step of this study. This will also enable the study of the relation between the upstream decay lengths and divertor power width at different collisionalities

In detached H-mode regimes, the near SOL electron density and temperature profiles are observed to broaden. This only happens when the divertor is completely detached when the effective collisionality is over a critical value. This phenomenon is similar to the one reported in earlier studies with L-mode plasmas, referred to as the L-mode high density transition. The fact that detachment, which is essentially a downstream phenomenon, affects the upstream profiles is curious. The mechanism responsible has not yet been established. As discussed in [19], a key element in the mechanism could be the convective transport associated with filaments: localized regions of plasma that propagate from the core into and through the SOL. Increased collisionality in the SOL would disconnect the filaments from the divertor and lead to enhanced convective transport. The enhanced upstream transport could either drive detachment downstream in the divertor or be driven by it.

In summary, the study of near SOL T_e decay length in attached H-mode regimes shows that a simple collisional relation is found to best relate the upstream decay lengths $\lambda_{T_{e,u}}$ and downstream divertor power widths, consistent with the two-point model. Log-linear regression shows that the SOL upstream dataset has the same main parametric dependencies as the scaling inferred from downstream Infrared camera measurements. In detached H-mode regimes, the broadening of the upstream decay lengths $\lambda_{T_{e,u}}$ is observed as a "shoulder" of density profile formed in SOL when the collisionality is over a critical value.

Acknowledgements

This work has been carried out within the framework of the EUROfusion Consortium and has received funding from the European Union's Horizon 2020 research and innovation programme under grant agreement number 633053. The views and opinions expressed herein do not necessarily reflect those of the European Commission.

References

[1] C. Pitcher and P.Stangeby, *Plasma Phys. Control. Fusion,* vol. 39, p. 779, 1997.

[2] P.C.Stangeby, The Plasma Boundary of Magnetic fusion devices, london: Institute of Physics Publishing, 2000.

[3] T. Eich et al, *Phys. Rev. Lett.,* vol. 107, p. 215001, 2011.

[4] T. Eich and e. al, *J. Nucl. Mater.,* vol. 438, p. S72, 2013.

[5] M. Makowski and e. al, *Phys. Plasmas,* vol. 19, p. 056122, 2012.

[6] T. Gray and e. al, *J. Nucl. Mater.,* vol. 415, p. S360, 2011.

[7] A. Thornton and e. al, *J. Nucl. Mater.,* vol. 438, p. S360, 2011.

[8] T. Eich et al, *Nucl. Fusion,* vol. 53, p. 093031, 2013.

[9] P. Stangeby, J. Canik and D. Whyte, *Nuclear Fusion,* vol. 50, p. 125003, 2010.

[10] B. Kurzan, *Rev.Sci.Instrum,* vol. 74, p. 4310, 2011.

[11] A.Herrmann, *Journal of Nuclear Materials,* Vols. 266-269, pp. 291-295, 1999.

[12] P. A. Schneider , *Plasma Phys. Control. Fusion,* vol. 54 , p. 105009, 2012.

[13] P. Schneider, Characterization and scaling of the tokamak edge transport barrier, 2012.

[14] A. Kallenbach and et al, *Plasma Phys. Control. Fusion,* vol. 46, p. 431, 2004 .

[15] J. Neuhauser, *Plasma Phys. Control. Fusion,* vol. 44, p. 855, 2002.

[16] B.LaBombard, *Phys.Plasma,* vol. 8, p. 2107, 2001.

[17] N. Asakura, *J.Nucl.Mater.,* vol. 241, p. 559, 1997.

[18] K.McCormick, *J.Nucl.Mater.,* Vols. 196-198, pp. 264-70, 1992.

[19] D.Carralero, *Nucl. Fusion,* vol. 54, p. 123005, 2014.

[20] H.Muller, in *21st PSI Conference, Kanazawa*, Japan, 2014.

[21] J. Mayra, *Phys. Plasma,* vol. 13, p. 112502, 2006.

[22] B. La Bombard, *Phys. Plasma,* vol. 18, p. 056104, 2011.

[23] C. S. Pitcher and e. al, *Plasma Phys. Control. Fusion,* vol. 39, p. 1129, 1997.

[24] R. J. Goldston, *Nucl. Fusion,* vol. 52, p. 013009, 2012.

[25] A. Kukushkin and e. al, *Contrib. Plasma Phys.,* vol. 40, p. 233, 2000.

[26] B. La Bombard, *Phys. Plasmas,* vol. 15, p. 056106, 2008.

[27] P. Snyder and e. al, *Phys. Plasmas,* vol. 16, p. 056118, 2009.